CBN 01-16

Apparatus for periodic magnetic structure tuning.

Alexander B. Temnykh

Laboratory of Nuclear Studies, Ithaca NY 14853, USA

September 21, 2001

Abstract

Devices with periodic magnetic structures such as wigglers and undulators are the key components of Free Electron Lasers, Synchrotron Radiation Sources and some types of RF power supplies. Any field imperfections along beam trajectory that distort periodicity of the magnetic field reduce operational performance of these devices. Thus, accurate measurement of magnetic field of these devise in order to localize and correct the field imperfection is very important issue.

The paper describes theory of new method based on vibrating wire technique adopted to magnetic measurement of periodic magnetic structure and reports test result. The test was done using a wiggler fabricated for Cornell High Energy Syncrotron Source with 7.8×10^3G of maximum magnetic field and 12cm period. The method demonstrated resolution of $\sim$ 1.0G (RMS) in the measurement of field imperfection and 2cm of spatial resolution.

1 Introduction

There are several methods commonly used for magnetic field measurement of periodic magnetic structures. Among them are field mapping with Hall probes, scanning with small searching coil and the pulsed wire technique. Some examples of application of these methods can be found elsewhere [1], [2], [3]. Each technique has it's own advantage and disadvantage.

[1]Work supported by the National Science Foundation

Mapping with Hall probe and scanning with searching coil can provide accurate field measurement but require complicated mechanical positioning systems and a good access to magnetic field region [1]. The large positioning systems needed for long magnetic structures can be quite expansive and requirement for good accessibility to the testing field region may constrain the magnet design. Another problem common for these methods is a baseline measurement ($zero$) drift which reduces precision.

The pulsed wire technique does not require special equipment and, because it uses as a probe a wire stretched through the testing magnetic field, the measurement setup can be made simple. However, distortion of the pulse signal propagating along the wire causes serious problem [4]. For this reason the technique can be used only for measurement of short magnetic structures. In addition, this method has very low accuracy.

The magnetic field measuring technique presented below is the vibrating wire method [5] adapted to a periodic magnetic structure. It is based on the following phenomenon. A taut wire of the length equal to the integer number of the magnetic structure periods is stretched inside of the structure. Then, the AC current with a resonance frequencies of the wire vibrating modes is applied. Lorentz forces between driving current and surrounding magnetic field will excite the wire vibrating modes, which are, in fact, a standing waves with length of $2L/n$, (L is the length of the wire, $n = 1, 2, 3, ...$). It will be shown in theoretical section that in perfect periodic magnetic structure, the forces can excite only modes with standing wave lengths equal to d, $d/2$, $d/3$ ..., where d is the magnetic structure period. Any field imperfection distorting periodicity will result in excitation of other, "not allowed", wire vibrating modes. Applying AC current at resonance frequencies of the restricted for perfect magnetic field modes and measuring amplitude and phase of wire vibration one can reconstruct distribution of error field along structure and correct the errors in location where they occurred.

In compare with the Hall probe and searching coil scanning, the method does not require expansive benches, it is more sensitive for magnetic field errors and has no problem with $zero$ drift. Like in the pulsed wire technique, the method uses as a probe a wire stretched through the testing field region. This makes measurement setup very simple and convenient for small aperture magnets. However, in contrast with pulsed wire the presented technique is much more accurate and can be used for measurement of long magnetic structures.

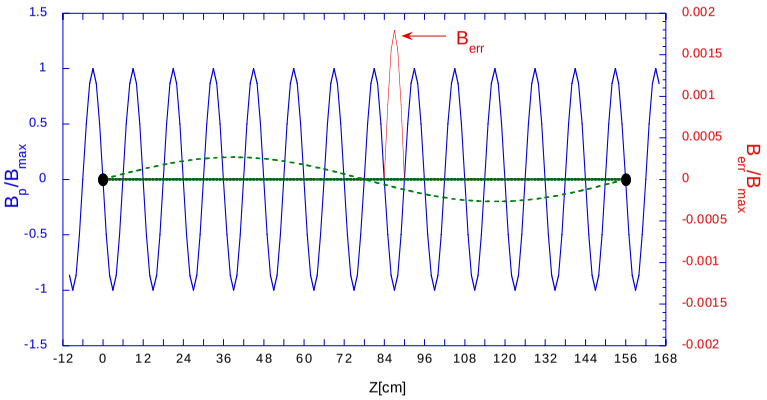

Figure 1: Model used in calculation. Shown are sinus-like ideal periodic magnetic field (left scale) and error field modeling single defective wiggler pole (right scale). Error field of 1.8×10^{-3} of amplitude of maximum wiggler field located at $z = 87$cm . Vibrating wire is shown by solid line, the second mode of the wire vibrating is depicted by dashed line. The wire length equals to 13 periods of magnetic structure. The wire ends are located at point with "zero" field.

In the paper theory of the method and result of the test experiments are presented.

2 Theory

2.1 Vibrating wire technique basic

Let $B(z)$ be a vertical magnetic field along periodic magnetic structure with period d. Suppose B(z) consists of two components - periodic (perfect) magnetic field $B_p(z)$ and error field $B_{err}(z)$:

$$B(z) = B_p(z) + B_{err}(z) \tag{1}$$

Consider the motion of the wire of length L, $L = Nd$ (N is integer number), stretched though the structure with tension T excited by AC current $I(t) = I_0 \exp(i\omega t)$ flowing through the wire. Schematic view of this model is given in Figure 1. Equation for the wire motion can be written as:

$$\mu\frac{\partial^2 X}{\partial t^2} = T\frac{\partial^2 X}{\partial z^2} - \gamma\frac{\partial X}{\partial t} + I(t)B(z) \tag{2}$$

Here $X(z,t)$ is the wire horizontal displacement, μ is the wire density per unit length. Terms $\sim \gamma$ and $\sim I(t)$ describe damping and Lorentz force. Elastic terms are neglected because assumed very thin wire, small amplitude of motion and long standing waves. Supposing wire ends are fixed we have:

$$X(z=0,t) = X(z=L,t) = 0 \tag{3}$$

Let's find solution $X(z,t)$ in form of sum of eigen modes, that satisfies the above condition:

$$X(z,t) = \sum_n X_n \sin(\frac{\pi n}{L}z)\exp(i\omega t) \tag{4}$$

Substituting (4) for (2) we yield equation for eigen modes amplitudes X_n:

$$\sum_n(\omega^2 - \omega_n^2 + i\gamma\omega)\sin(\frac{\pi n}{L}z)X_n = \frac{I_0}{\mu}B(z) \tag{5}$$

where

$$\omega_n = \frac{\pi n}{L}\sqrt{\frac{T}{\mu}} \tag{6}$$

Note that ω_n are eigen-frequencies of the wire vibrating modes. Equation (5) can be easily resolved relative to X_n by multiplying both sides by $\sin(\frac{\pi n}{L}z)$ and integrating over the wire length. This gives:

$$X_n = \frac{I_0}{\mu}\frac{1}{(\omega^2 - \omega_n^2 + i\gamma\omega)}B_n \tag{7}$$

where

$$B_n = \frac{2}{L}\int_0^L B(z)\sin(\frac{\pi n}{L}z)dz = \frac{2}{L}\int_0^L (B_p(z) + B_{err}(z))\sin(\frac{\pi n}{L}z)dz \tag{8}$$

Equations (7) and (8) express the basic idea of vibrating wire field-measuring technique. One can see that the amplitude of eigen mode, X_n, excited by Lorentz forces is proportional to the corresponding harmonic of sine Fourier transform of the field along wire, B_n. Thus by measuring X_n one can find B_n and reconstruct the field using inverse transformation:

$$B(z) = \sum_n B_n \sin(\frac{\pi n}{L}z) \tag{9}$$

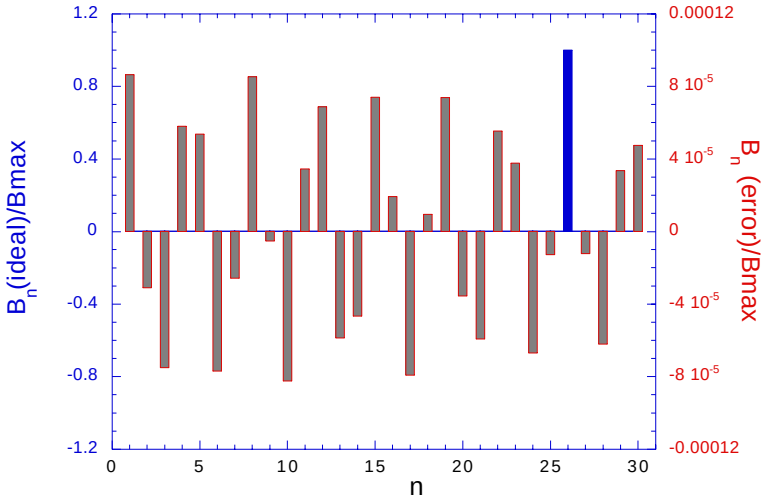

Figure 2: Ideal periodic field harmonic (solid bar, left scale) and harmonics of error field (hatched bars, rigt scale) for the model depicted in Figure 1

2.2 Error Field and Periodic Field Harmonics Content

Let's compare harmonics contents of periodic and error fields. If the wire length is equal to integer number of structure periods and wire ends are located at points of "zero" field as shown on Figure 1, then according to equation (8) the lowest order of harmonic of periodic field will be $n_l = 2N$ (for the depicted model $n_l = 26$). If the field is sinus function, then this will be only one harmonic. If the field is periodic but not a sinus function, the orders of the other harmonics will be multiple to n_l, i.e., $n = 2n_l, 3n_l, ...$ In contrast, Fourier harmonics of the error field, can be of any order starting from 1. Figure 2 shows result of calculation for the model depicted on Figure 1. Here is one harmonic of the ideal periodic field ($B_{n=26}$) and verity of the error field harmonics. The difference in harmonic contents of periodic and error fields suggests a very simple selective method of the error field measurement. One can measure harmonics "restircted" for the ideal periodic field, that will be error field harmonics, and then use these to reconstruct the error field. This approach is illustrated on Figure 3. Here solid line represents result of error field reconstruction using 16 lowest order harmonics, dotted line shows original error field. One can see that although reconstructed field amplitude and the peak width are different from the original, the peak lo-

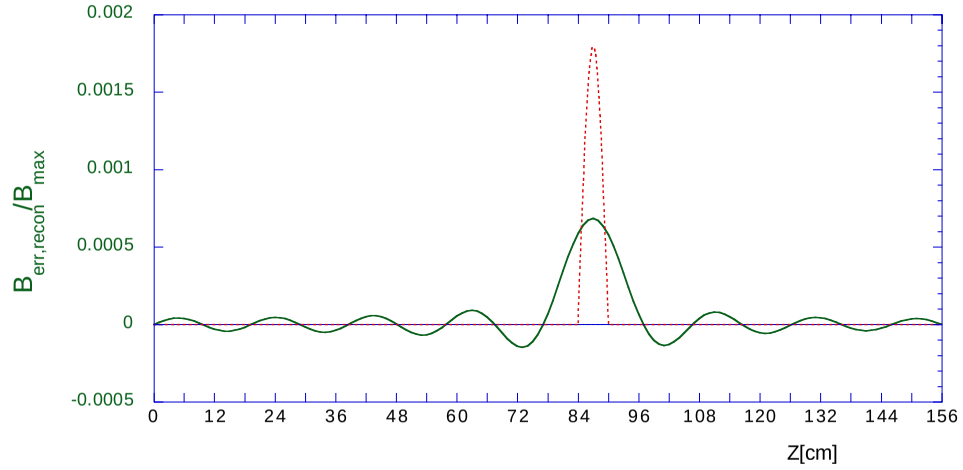

Figure 3: Original error field (dotted line) and the field reconstructed by using 16 low order harmonics (solid line). One division on horizontal axiss corresponds to a halve period (one pole) of wiggler used in experiments.

cation evidently points at the location of error field at $z \sim 87$cm. The peak width (resolution in z direction) and the peak amplitude depend on number of harmonics used for reconstruction.

Note that the error field harmonics are ~ 4 order of magnitude smaller then the main field harmonic. However, because the corresponding harmonics of the wire vibrating modes are well separated in frequency domain and have low damping rate γ, it is possible to measure the small error field in the presence of the strong main field.

The next section discusses some details of the harmonics measurement.

2.3 Harmonics measurement method

The general solution for wire motion $X(z,t)$ can be written in form:

$$X(z,t) = \frac{I_0}{\mu} \exp(i\omega t) \sum_n \frac{1}{\omega^2 - \omega_n^2 + i\gamma\omega} \sin(\frac{\pi n}{L} z) B_n \qquad (10)$$

Assume there is wire position sensor located at $z = z_0$ and we measure parameter $\mathcal{F}(\omega)$ which is averaged over the time product of the wire position given by the sensor, $X(z = z_0, t)$, and the current driven through the wire,

$I_0\, exp(i\omega t)$:

$$\mathcal{F}(\omega) = \frac{1}{T}\int_0^T X(z_0,t)I(t)dt = \frac{I_0^2}{2\mu}\sum_n \sin(\frac{\pi n}{L}z_0)\frac{(\omega-\omega_n)}{4\omega(\omega-\omega_n)^2+\omega\gamma^2}B_n \quad (11)$$

Note that $\mathcal{F}(\omega)$ is similar to a sine component of lock-in-amplifier signal with a driving current used as a reference. If driving current frequency is closed to one of the eigen mode frequencies ($\omega \sim \omega_n$) due to resonant denominator n-th term will dominate in sum (11), i.e.,

$$\mathcal{F}(\omega) \simeq \frac{I_0^2}{2\mu}\sin(\frac{\pi n}{L}z_0)\frac{(\omega-\omega_n)}{4\omega(\omega-\omega_n)^2+\omega\gamma^2}B_n \quad (12)$$

for

$$\omega \sim \omega_n \quad (13)$$

For each measured harmonic the driving current frequency has been scanned through the resonant frequency of n-th mode of the wire vibration and the measured function $\mathcal{F}(\omega)$ has been fitted with formula:

$$\mathcal{F}(\omega) = \frac{I_0^2}{2\mu}\sin(\frac{\pi n}{L}z_0)\frac{(\omega-\mathcal{A})}{4\omega(\omega-\mathcal{A})^2+\omega\mathcal{C}^2}\mathcal{B}+\mathcal{D} \quad (14)$$

Where coefficients $\mathcal{A}, \mathcal{B}$ and $\mathcal{C}$ are free parameters corresponding to ω_n, B_n and γ. Parameter $\mathcal{D}$ has been added to describe non-resonance coupling between driving current and signal from wire position sensor. The coupling can be a result of parasitic electrical coupling between connectors or due to non-resonance terms presented in formula (11). Other parameters (I_0, μ, L and z_0) are well defined. Harmonics B_n obtained from the fit had been used for the field reconstruction.

3 Test

3.1 Test Setup

The model discussed in previous sections and depicted in Figure 1, in fact, represents the setup used in the test.

For the test measurements there was used the wiggler recently built for Cornell High Energy Synchrotron Source. The wiggler's general parameters are given in Table 1.

Length [m]	3.0
Number of poles	50
Period [cm]	12.0
Peak magnetic field [T]	0.780
Gap [cm]	4.0
Pole width [cm]	11.0

Table 1: General parameters the wiggler used in measurements.

The built vibrating wire (VW) probe is schematically shown in Figure 4. The length of the wire section enable to vibrate was 156cm which equals to 13 wiggler periods. The fundamental vibrating mode frequency was $\omega_1 \approx 2\pi \times 30$Hz, typical amplitude of driving current $I_0 \approx 70$mA and damping rate $\gamma \sim 1\text{sec}^{-1}$. The sag estimated from the frequency was 0.34mm. As a wire position detector a "Π" shaped opto-electronic assembly H21A1 (Newark Electronics) consisting of a light-emmiting-diode (LED) on one leg and photo-transistor on other was used. The light flux detected by photo-transistor is very sensitive to horizontal wire position. Wave form generator "HP33120A", controlled by computer Macintosh Quadra 800, was used to drive current through the wire. A "LAB-NB" board installed in the computer and programs based on "Lab-View" software provided all needed signals proceedings. To carry out test experiments, VW probe was inserted in the wiggler gap, so the taut wire was aligned with a wiggler center line and wire ends were positioned between poles in regions where vertical magnetic field is close to zero. Two types of experiments described below were performed.

3.2 Measurement of "calibrated" field distortion

In the first experiment, there was measured a wiggler field distortion resulted from placing of small (2×2cm, 0.1mm thikness) μ-metal shims in the wiggler gap at different locations. The shims were placed, first, at $z = 87$cm then at $z = 117$cm, z starts from wire end. The amplitude of the field distortion was estimated as $\sim$ 14G or $\sim 1.8 \times 10^{-3}$ of maximum wiggler field. The estimation was done using change in the vertical field integral measured with a long flipping coil and assuming that the length of the region where field

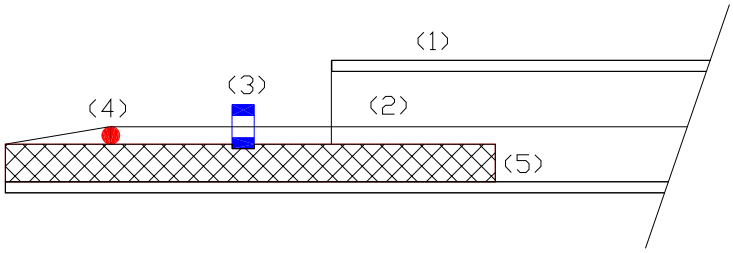

Figure 4: Cross section of the VW probe used in the test. One end of the probe is shown. Inside of 2cm OD plastic tubing (1), 100 μm copper-beryllium wire (2) was taut. The wire ends were fixed on spacers (5), position of 2mm diameter G-10 cylinders (4) defined the length of the vibrating wire equal to 13 wiggler periods. A phototransistor-LED assembly (3) located at 30mm from the wire fixed point was used to detect horizontal wire motion.

was distorted is a halve of the wiggler period $\sim$ 6cm as shown in Figure 1. 16 lowest order harmonics with and without the shims were measured with VW probe. The difference in the harmonics was used to reconstruct the field change. Results of this experiment are presented in Figure 5. Here three plots show the reconstructed field distortion (solid line), model calculation (dashed line) made in previous section and difference between measurement and calculation (dotted line). To facilitate analysis, the modeled and measured field distortions were scaled to have the same peak amplitudes equal to estimated field distortion.

There is a very good consistency between measured and calculated field distortions in both cases. The measured locations of maximum field distortion 85.7cm and 117.0cm reveal with assurance the shim locations at 87.0cm and 117cm. Comparing measured and real locations of the field distortion one can estimate the spatial resolution of the method to be better than 2cm. The RMS residual between measured data and model (the noise) in both cases $\sim 1.5 \times 10^{-4}$ of maximum wiggler field. This is much better than one can expect from commonly used Hall probe measurement.

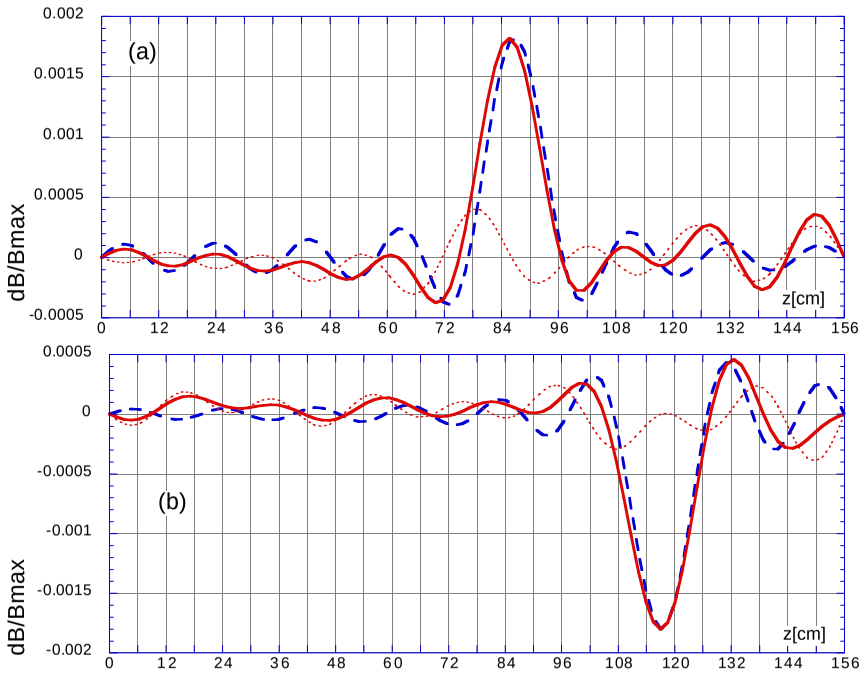

Figure 5: Measured (solid line), modeled (dashed line) and residual (dotted line) between measured and modeled field distortion resulted from μ-metal shim inserted in wiggler gap. Vertical scale is in units of maximum wiggler field. (a) Shim placed at $z = 87$cm, measured location of maximum field distortion $z = 85.72$cm, RMS residual between modeled and measured distortion $\sim 1.4 \times 10^{-4}$. (b) Shim placed at $z = 117$cm, measured location of maximum field distortion $z = 117.0$cm, RMS residual $\sim 1.5 \times 10^{-4}$.

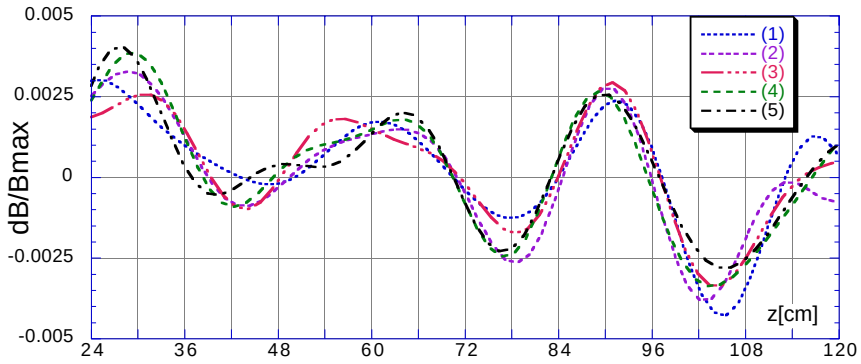

Figure 6: Reconstructed wiggler error field measured by VW probe placed at different position along magnet. Horizontal axis gives z coordinate along wiggler. Plots (1), (2), (3), (4) and (5) correspond to VW probe position with probe end located next to pole 10, 11, 12, 13 and 14 (numbering starts from wiggler's North end).

3.3 Measurement of the wiggler error field

The goal of the next experiment was to measure the wiggler error field. Results are shown in Figure 6. To ensure that the measured data relate to wiggler error field but not to systematic errors due to measuring technique, there were made 5 measurements at different VW probe position along the wiggler. Five plots in Figure 6 show reconstructed error field in common for all these measurements region. Here coordinate z is given relative to wiggler but not to the wire. The observed correlation between reconstructed field for different measurements and z reassures that the measured error field distribution is related to the magnet. Amplitude of the error field, $\sim 2.5 \times 10^{-3}$ of the maximum wiggler field, revealed by the measurements can be easily explained by the wiggler poles geometry variation or by variation of magnetization strength of permanent magnets.

Conclusion

Vibrating wire technique was adapted for measurement of imperfections of periodic magnetic structures. Based on developed theory, the VW probe was built and test experiments were carried out. The probe demonstrated RMS

$\sim 1.5 \times 10^{-4}$ of maximum wiggler field sensitivity to the non-periodic field imperfection and better than 2cm spatial resolution.

The sensitivity and spatial resolution of the method can be significantly improved by optimizing the wire properties, by measuring more harmonics and by vacuum encapsulating of the vibrating wire. The latter will decrease air friction leading to lower damping rate and higher sensitivity.

The transfers dimensions of VW probe can be reduced to less then 1mm scale without any other parameters degradation. That will enable the use of the described technique for precise tuning of miniature magnetic structures with small aperture.

References

[1] J. Pfluger, Insertion Devices for 4^{th} Generation Light Sources. Proceedings of the 1999 Particle Accelerator Conference, New York, 1999, pp. 157-161.

[2] J. Pfluger, Rev. Sci. Instrum. 63,1 (1992), 295

[3] J. G. Melton, M. J. Burns, D. J. Honaberger, Pulsed Taut-Wire Measurement of the Magnetic Alignment of the ITS Induction Cells, Proceedings of the 1993 Particle Accelerator Conference, Washington, D.C., 1993, pp. 2944-2946.

[4] R. W. Warren, Limitations on the use of the pulsed-wire field measuring technique, Nuc. Inst., A 272 (1988) 257 - 263.

[5] A. Temnykh, Vibrating wire field-measuring technique, Nuc. Inst., A 399 (1997) 185-194